



**LEVEL II**



RADC-TR-78-158  
Phase Report  
July 1978

**A FUNDAMENTAL STUDY OF THE ELECTROMAGNETIC  
PROPERTIES OF ADVANCED COMPOSITE MATERIALS**

W. J. Gajda

Syracuse University

AD A059029

Best Available Copy

This report has been reviewed by the NADC Information Office (OI) and is releasable to the National Technical Information Service (NTIS). It will be releasable to the general public, including foreign nations.

ADP-TR-78-158 has been reviewed and is approved for publication.

APPROVED:



ROY E. STRATTON  
Project Engineer



Best Available Copy

UNCLASSIFIED

SECURITY CLASSIFICATION OF THIS PAGE (When Data Entered)

REPORT DOCUMENTATION PAGE		READ INSTRUCTIONS BEFORE COMPLETING FORM
1. REPORT NUMBER RADC-TR-78-158	2. GOVT ACCESSION NO.	3. RECIPIENT'S CATALOG NUMBER
4. TITLE (and Subtitle) FUNDAMENTAL STUDY OF THE ELECTROMAGNETIC PROPERTIES OF ADVANCED COMPOSITE MATERIALS	5. TYPE OF REPORT & PERIOD COVERED Phase Report 1 Oct 76 - 30 Sep 77	
7. AUTHOR(s) W. J. Gajda	6. PERFORMING ORG. REPORT NUMBER N/A	
9. PERFORMING ORGANIZATION NAME AND ADDRESS Syracuse University Syracuse NY 13210	8. CONTRACT OR GRANT NUMBER(s) F30602-75-C-0121	
11. CONTROLLING OFFICE NAME AND ADDRESS Rome Air Development Center (RBCT) Griffiss AFB NY 13441	10. PROGRAM ELEMENT, PROJECT, TASK AREA & WORK UNIT NUMBERS 61101F 01747T03	
14. MONITORING AGENCY NAME & ADDRESS (if different from Controlling Office) Same	12. REPORT DATE July 1978	
16. DISTRIBUTION STATEMENT (of this Report) Approved for public release; distribution unlimited. 52 p.	13. NUMBER OF PAGES 44	
17. DISTRIBUTION STATEMENT (for the abstract entered in Block 20, if different from Report) Same	15. SECURITY CLASS. (of this report) UNCLASSIFIED	
18. SUPPLEMENTARY NOTES RADC Project Engineer: Roy F. Stratton (RBCT) *Work done by Prof. W. Gajda at Notre Dame University under subcontract with Syracuse University.	15a. DECLASSIFICATION/DOWNGRADING SCHEDULE N/A	
19. KEY WORDS (Continue on reverse side if necessary and identify by block number) Advanced composite materials      Doping Permittivity                              Modeling Permeability                                Graphite Conductivity                                Boron	16. DISTRIBUTION STATEMENT (of this Report) Approved for public release; distribution unlimited. 52 p.	
20. ABSTRACT (Continue on reverse side if necessary and identify by block number) This report covers an effort to understand, model and modify the fundamental electrical properties of advanced composite materials, specifically graphite/epoxy and boron/epoxy. The electrical properties of graphite and boron fibers and of epoxy were measured. The anisotropic conductivity of boron fibers was studied. Models were developed which predicted the electrical properties of the composites--with reasonable accuracy for some cases. The conductivity of graphite fibers was increased about a factor of 50 (to 10 <sup>6</sup> ohms/meter) by doping	17. DISTRIBUTION STATEMENT (of this Report) Approved for public release; distribution unlimited. 52 p.	

DD FORM 1473  
1 JAN 73

UNCLASSIFIED

SECURITY CLASSIFICATION OF THIS PAGE (When Data Entered)

640 H4 1

101

UNCLASSIFIED

SECURITY CLASSIFICATION OF THIS PAGE (When Data Entered)

with boron; the conductivity of boron fibers was increased about a factor of  $10^3$  by doping with carbon.

ACCESSION for	
NTIS	White Section <input checked="" type="checkbox"/>
DDC	Buff Section <input type="checkbox"/>
UNANNOUNCED	<input type="checkbox"/>
JUSTIFICATION	
BY	
DISTRIBUTION/AVAILABILITY CODES	
Dist. Avail. and/or SPECIAL	
A	

UNCLASSIFIED

SECURITY CLASSIFICATION OF THIS PAGE (When Data Entered)

## PREFACE

This effort was conducted by Notre Dame University subcontracting through Syracuse University under the sponsorship of the Rome Air Development Center Post-Doctoral Program for Rome Air Development Center. Dr. Roy F. Stratton, RADC/RBCT, was project engineer and provided overall technical direction and guidance.

The RADC Post-Doctoral Program is a cooperative venture between RADC and some sixty-five universities eligible to participate in the program. Syracuse University (Department of Electrical Engineering), Purdue University (School of Electrical Engineering), Georgia Institute of Technology (School of Electrical Engineering), and State University of New York at Buffalo (Department of Electrical Engineering) act as prime contractor schools with other schools participating via sub-contracts with prime schools. The U.S. Air Force Academy (Department of Electrical Engineering), Air Force Institute of Technology (Department of Electrical Engineering), and the Naval Post Graduate School (Department of Electrical Engineering) also participate in the program.

The Post-Doctoral Program provides an opportunity for faculty at participating universities to spend up to one year full time on exploratory development and problem-solving efforts with the post-doctorals splitting their time between the customer location and their educational institutions. The program is totally customer-funded with current projects being undertaken for Rome Air Development Center (RADC), Space and Missile Systems Organization (SAMSO), Aeronautical System Division (ASD), Electronic Systems Division (ESD), Air Force Avionics Laboratory (AFAL), Foreign Technology Division (FTD), Air Force Weapons Laboratory (AFWL), Armament Development and Test Center (ADTC), Air Force Communications Service (AFCS), Aerospace Defense Command (ADC), Hq USAF, Defense Communications Agency (DCA), Navy, Army, Aerospace Medical Division (AMD), and Federal Aviation Administration (FAA).

Further information about the RADC Post-Doctoral Program can be obtained from Mr. Jacob Scherer, RADC/RBC, Griffiss AFB, NY, 13441, telephone Autovon 587-2543, Commercial (315) 330-2543.

178 08 15 015

## TABLE OF CONTENTS

1) <u>INTRODUCTION</u> .....	1
2) <u>Current in Composites</u> .....	3
3) <u>Elements of Microscopic Fiber Conductivity and Impurity Diffusion</u> ...	12
4) <u>Graphite Fibers</u> .....	16
5) <u>Boron Fibers</u> .....	19
6) <u>Diffusion Experiments</u> .....	31
7) <u>Electrical Behavior of Diffused Fibers</u> .....	35
8) <u>Summary of Results and Conclusions</u> .....	39
9) <u>ACKNOWLEDGMENTS</u> .....	39
<u>REFERENCES</u> .....	40
<u>APPENDIX A</u> .....	42

### LIST OF ILLUSTRATIONS

	Page
Figure 1 Model for Determination of $\sigma_L$ .....	5
Figure 2 Model for Determination of $\sigma_T$ .....	6
Figure 3 Random Fiber Model.....	9
Figure 4 Current Constriction Model.....	18
Figure 5 Boron Fiber Contact Geometry.....	20
Figure 6 I-V Characteristics of Boron Fibers with Indium Contacts....	20
Figure 7 Indium Contact to Fiber Core.....	22
Figure 8 Indium Isolated from Core.....	22
Figure 9 Geometry for Calculation of $\sigma_B$ .....	23
Figure 10 Sample Geometrics.....	25
Figure 11 Conductivity ~ Temperature Profile.....	29
Figure 12 Boron Fiber R-T Curve.....	30
Figure 13 Boron Fiber Energy Gap.....	31
Figure 14 Basic Diffusion Furnace.....	32
Figure 15 Conductivity Enhancement in Graphite.....	37
Figure 16 Conductivity Enhancement in Graphite, High Temperature Diffusion.....	38
Figure 17 Conductivity Enhancement in Boron.....	38

## 1) INTRODUCTION

Advanced composite materials have begun to be more widely used as structural and surface components in modern aircraft. Immediate questions arise concerning the effects of lightning upon composite structures, the shielding effectiveness of the materials against electromagnetic interference and electromagnetic pulse effects, the radar cross-section and precipitation static effects.

Research has shown that composites are more likely than metals to degrade structurally under simulated lightning excitations<sup>1</sup> and that the electrical shielding effectiveness of typical composites (graphite/epoxy, boron/epoxy and Kevlar/epoxy) is less than that of metals over the range of frequencies DC to 3 GHz,<sup>2,3</sup> although the shielding effectiveness of graphite/epoxy approaches that of metals for frequencies above 100 MHz.

Partial solutions to the problems of lightning susceptibility and shielding have involved conductive coatings, embedded conductive grids and diverter strips.

However, a more fundamental approach could offer significant advantages. To anyone concerned with the problem of shielding the interior of a vehicle against electromagnetic hazards, the possibility of a material with the specific strength of a graphite/epoxy or a boron/epoxy composite and the conductivity of aluminum is appealing. In order to improve the shielding effectiveness and lightning strike resistance of these materials, it is natural to consider ways in which the electrical conductivity and/or permeability can be increased without significant decreases in specific strength.

A necessary prelude to developing such materials is a determination of the fundamental mechanisms responsible for the electrical behavior of composites. Previous work<sup>4</sup> indicates that low frequency conductivity depends on fiber conductivity and fiber-to-fiber contact. This leads to the possibility of increasing fiber conductivity by doping techniques. For example, polycrystalline boron is a semiconductor and it should be possible to identify dopants which, when added to the fibers in parts per billion concentrations, result in orders of magnitude increase in fiber and composite conductivity. Polycrystalline carbon is less well characterized electrically but, in view of carbon's position in the fourth group of the periodic table, doping should be possible in this material also.

Permeability increases would improve shielding effectiveness and could be accomplished by doping composite fibers with atoms of high magnetic moment. Increases in mass density are a possible problem with this approach and increased permeability would not improve response to lightning.

Further, such doping of fibers should add little to composite fabrication costs because it could probably be accomplished by simply changing the gas mixture in which the fibers are formed (either by graphitization of a hydrocarbon precursor or by chemical vapor deposition of boron on tungsten).

To examine these ideas, a research program was initiated with the following three general goals:

- 1) Characterize the electrical behavior of as-manufactured graphite and boron fibers by measuring the low frequency conductivity,  $\sigma$ . This task requires developing reliable techniques of making ohmic electrical contact to the fibers.
- 2) Experimentally and theoretically determine the fundamental physics of current flow in advanced composite materials; in particular, if the polycrystalline fibers are semiconductor-like, what elements could be used to dope the fibers to change their electrical conductivity?
- 3) Experimentally investigate various doping methods to increase the intrinsic conductivities of composites.

The following specific tasks were accomplished during the year. Techniques were developed for making electrical contact to graphite and boron fibers and the DC electrical conductivities of fibers provided by three manufacturers (Narmco and Hercules (graphite) and Avco (boron)) were measured. Diffusions of boron into graphite fibers and carbon into boron fibers were carried out and the resultant changes in electrical conductivity were measured. The high field non-linear thresholds of the fibers were measured in order to assess failure mechanisms under high-level electrical excitation. Models were formulated to allow the prediction of composite conductivities based on the conductivities of the constituent fibers and matrix. It was theoretically concluded that attempts to increase the magnetic permeabilities of advanced composite materials would result in unacceptable decreases in specific strength and this approach was not investigated experimentally. Such a specific strength decrease will result from the mass density increase as relatively dense high permeability materials are added. For example, loading the composite with 10 volume percent high permeability iron-nickel alloy would increase the composite density by 40% - a change which would be unacceptable in many applications although the relative permeability would be 20.

The next section of this report develops simple models of current flow in advanced composites. The large differences in the conductivities of graphite/epoxy and boron/epoxy are demonstrated and the central role played by the fibers in determining overall material conductivity is illustrated. These results indicate that increasing fiber conductivity will indeed lead to high composite conductivities. Although such materials would have to be thoroughly tested, a comparison of the responses of metals and presently manufactured advanced composites to electromagnetic hazards indicates that enhanced composite conductivities would lead to reduced electromagnetic vulnerability.

Section 3 introduces the theory of impurity diffusion in cylindrical geometries germane to fibers.

The experimental investigations of as-manufactured graphite and boron fibers are discussed in Sections 4 and 5 respectively. Techniques used to characterize, clean and form electrical contacts are described. The DC electrical conductivities and anisotropies associated with the fibers are determined.

The experimental techniques used to introduce impurities into the fibers are detailed in Section 6. Thermal diffusion was used for both boron and

graphite while the intercalation of super-acid radicals into graphite was also investigated. The results of these processes are given in Section 7.

The last section summarizes the progress made and indicates the directions along which the research will continue.

## 2) CURRENT IN COMPOSITES

The materials considered in this report are inhomogeneous, consisting of arrays of fibers (each fiber, in general, electrically anisotropic) in a matrix (electrically isotropic for all materials presently under investigation). The theoretical situation is worsened by the lack of periodicity which precludes the use of translational invariance symmetry as commonly applied in the theory of crystalline solids.

It is possible to identify two major lines of analysis of such materials. The first may be termed the statistical study of inhomogeneous materials and has been developed primarily by individuals studying problems of heat flow in disordered media (thermal insulation, for example). The basic theme is the determination of upper and lower bounds of the transport coefficients (thermal conductivity, electrical conductivity, ...), in terms of the properties of the two phases and the volume fractions of each phase. Although such models have been developed primarily for solids consisting of spheres dispersed in a matrix, extensions<sup>3</sup> have been published for dispersions of fibers. It must be noted that the theoretical analyses do not assume any touching between the fibers but rather assert that each fiber is surrounded by the matrix material.

We begin by examining the applicability of these bounds to the case of graphite fibers in either an epoxy or a polyimide matrix. It is most convenient to examine the ratio of the upper bound ( $\sigma_U$ ) to the lower bound ( $\sigma_L$ ). The general expression takes the form<sup>5</sup>

$$\sigma_U/\sigma_L = \alpha^{-1} [1 + \alpha f - A] / [f + \alpha (1-f) + B]$$

with

$$A = .5\alpha f(1-f) / [f + 2G_1(1-f)^2 - 2G_2f^2]$$

$$B = .25 \alpha f(1-f) / [f^2G_2 - (1-f)^2G_1]$$

where  $\alpha$  is the ratio of fiber to matrix conductivities,  $f$  the volume fraction of the fibers and  $G_1, G_2$  are empirical shape factors (see below).

In writing the above equation, available experimental evidence indicating that fiber conductivities are several orders of magnitude greater than matrix conductivities was invoked. As long as neither  $f$  nor  $1-f$  closely approaches zero (a condition which is satisfied in both typical graphite/epoxy and graphite/polyimide samples), the bounds ratio ( $\sigma_U/\sigma_L$ ) simplifies further and numerical values for the shape factors may also be substituted.<sup>6</sup>

$$G_1 = G_2 = 0.25$$

For a sample of graphite/epoxy or graphite/polyimide representative of the materials used in aircraft, the following approximate numerical values apply.

$$f = 0.7, \quad \sigma_1 = 10^4 \text{ mhos/meter}, \quad \sigma_2 = 10^{-8} \text{ mhos/meter}$$

The bounds may be evaluated directly as

$$\frac{\sigma_U}{\sigma_L} = 4.41(10^{10})$$

This value is significantly greater than the experimentally measured values.

$$\frac{\sigma_U}{\sigma_L} = 200.$$

It may be concluded that these Beran-Silnutzer bounds are not sufficiently tight to realistically predict the electrical properties of graphite/resin composites. Although the bounds are valid, they are more than ten orders of magnitude apart and are of little value in predicting the conductivities to be expected in a given composite. These results imply that the basic divergence between this theory and experiment involves the theoretical neglect of fiber-to-fiber contact. This contact is a dominant feature in configurations in which current is directed orthogonal to the fiber axis and cannot be ignored if useful bounds are to be derived theoretically.

The second approach to the analysis of the electrical properties of composites rests upon deterministic models in which one attempts to solve for the precise distributions of currents in a sample excited by an external voltage and, in this way, determine an effective conductivity for the material. Such models become intractable when large numbers of fibers must be considered but insight can be obtained into the basic electrical behavior by examining a few simple models.

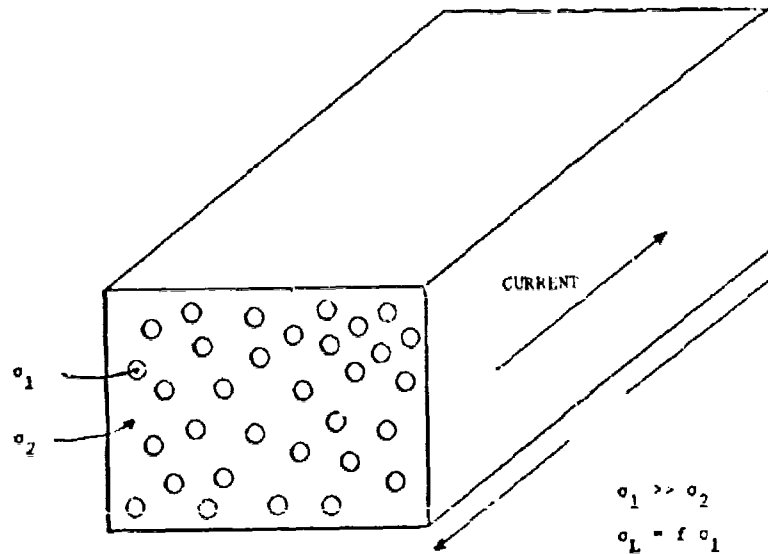
We begin our development of such models of electrical conductivity in advanced composites by considering the most simple system--the unidirectional, single-ply system. If care is taken to abrade any epoxy-rich regions from the upper and lower surfaces of such a sample, we find that the conductivity may be characterized by two quantities:  $\sigma_L$ , the value associated with current along the fiber axis and  $\sigma_T$ , the value associated with current orthogonal to the fiber axis (either from top to bottom or in the sample plane at right angles to the fibers).

We use the symbol  $f$  to denote the volume fraction of fibers in the unidirectional sample,  $\sigma_1$  for the fiber conductivity and  $\sigma_2$  for the epoxy matrix conductivity. For current in the longitudinal direction (along the fibers), the total sample conductance (Figure 1) is simply the summation of the conductances of the individual fibers plus the conductance of the epoxy. This may be written as

$$G = \frac{\sigma_1 f A}{L} + \frac{\sigma_2 (1-f) A}{L}$$

from which it follows that the longitudinal conductivity may be written as

$$\sigma_L = \sigma_1 f + \sigma_2 (1-f)$$



MODEL FOR DETERMINATION OF  $\sigma_L$

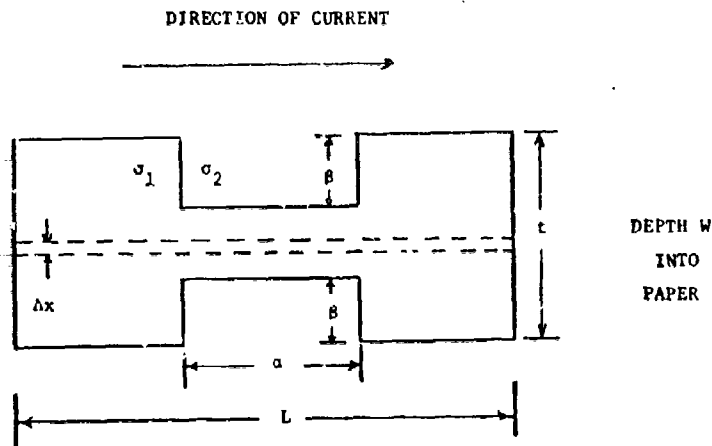
FIGURE 1

Although minor deviations from this result are observed in some unidirectional samples primarily as a result of breaks in fibers and skewing of fibers from the longitudinal axis, it yields acceptable results. For example, the DC conductivity of 'typical' graphite fibers has been measured<sup>7</sup> as  $2(10^4)$  mhos/m. (Section 4). For unidirectional samples with a fiber volume fraction of 0.6, the above equation predicts the longitudinal conductivity to be

$$\begin{aligned} \sigma_L &= 2(10^4)(0.6) + \sigma_2(0.4) \\ &= 1.2(10^4) \text{ mhos/m.} \end{aligned}$$

The second term is, of course, negligible when the matrix is epoxy. This value is in excellent agreement with low frequency experimental measurements<sup>7</sup> (DC to 5 MHz), which have been in the range of  $1-2(10^4)$  mhos/m for unidirectional samples.

The calculation of the transverse conductivity  $\sigma_T$  is significantly more difficult. In order to develop insight into this problem, consider a simple composite composed of two fibers with rectangular cross-sections, which touch each other via a rectangular "neck." This model is shown in Figure 2.



MODEL FOR CALCULATION OF  $\sigma_T$

FIGURE 2

Consider a slab (thick, depth W and length L) of this sample as sketched in Figure 2. The conductance of this section can be calculated directly as

$$\Delta G = \sigma_1 W \Delta x / L \quad \text{for} \quad -\frac{t}{2} + \beta < x < \frac{t}{2} - \beta$$

$$\Delta G = \sigma_1 \sigma_2 W \Delta x / (\sigma_1 \alpha + \sigma_2 (L - \alpha)) \quad \text{otherwise}$$

The various geometric terms are defined in Figure 2.  $\alpha$ ,  $\beta$  are used to define the 'neck' connecting the two fibers as shown in the figure.

The total conductance is

$$G = \int_{G(-t/2)}^{G(+t/2)} dG = \frac{\sigma_1 W t}{L} + \left[ \frac{\sigma_1 \sigma_2 W}{\sigma_1 \alpha + \sigma_2 (L - \alpha)} - \frac{\sigma_1 W}{L} \right] (2\beta)$$

This result may be rewritten in terms of a transverse conductivity  $\sigma_T$ , defined as

$$G = \sigma_T t W / L,$$

which implies that

$$\sigma_T = \sigma_1 (1 - 2\beta/t) + \frac{\sigma_1 \sigma_2 (2\beta/t)}{\sigma_1 (\alpha/L) + \sigma_2 (1 - \alpha/L)}$$

When  $\beta \rightarrow t/2$  and  $\alpha \rightarrow L$ , the model simplifies to pure matrix and the conductivity takes the form

$$\sigma_T = \sigma_1 (1 - 1) + \sigma_1 \sigma_2 / (\sigma_1 + \sigma_2 (0)) = \sigma_2.$$

When  $\beta \rightarrow 0$  and  $\alpha \rightarrow 0$ , the model simplifies to pure fiber and the conductivity is

$$\sigma_T = \sigma_1 \quad \text{as expected.}$$

The general expression for  $\sigma_T$  is of interest because of the information it contains about the situation in which the fibers do not touch. This is described by the geometric condition  $\beta = t/2$ , and the equation for transverse conductivity reduces to

$$\sigma_T = \sigma_2 (L/\alpha).$$

The low probability of non-touching fibers in graphite/epoxy materials is demonstrated by experimental results. The transverse conductivity for graphite/epoxy has been measured to have a value of 200 mhos/m., while the quantity  $L$  is approximately  $2(10^{-5})$ m. Estimating the conductivity of the epoxy matrix to be  $10^{-8}$  mhos/m yields

$$\alpha = 1(10^{-15}) \text{ m.}$$

Such a small separation is, for all meaningful purposes, equivalent to contact between fibers and it may be concluded that, in a transverse sample of graphite/epoxy, fiber-to-fiber contact is essential to describe the conduction of charge in directions orthogonal to the fiber axis.

It is important to note that such fiber contact does not occur in boron/epoxy and, in these materials, the flow of charge across fibers is limited by the conductivity of the epoxy matrix. In unidirectional samples of boron/epoxy<sup>7</sup>,  $\sigma_L = 30$  mhos/m and  $\sigma_T = 2(10^{-8})$  mhos/m.

In composites which have an insulating matrix, two factors determine the conductivities of unidirectional samples; the fiber conductivity and the degree of fiber contact. For multiple-ply lay-ups, a simple model<sup>7</sup> describing the overall conductivity  $\sigma$  is given by the equation

$$\sigma = \frac{1}{N} \sum_{i=1}^N \sigma_i$$

where  $N$  is the number of layers and  $\sigma_i$  is the conductivity in the direction of interest of the  $i^{\text{th}}$  layer. This equation follows from the assumptions that the conductances of the layers may be treated as effectively in parallel and that each ply has the same thickness.

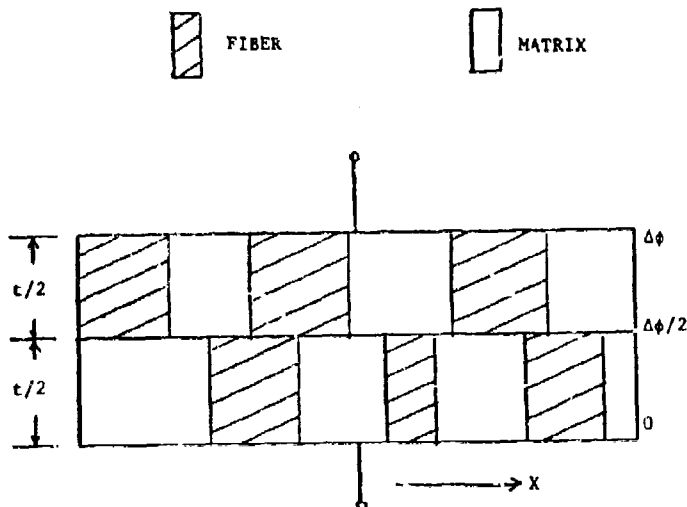
All of these results pertain to situations in which current is moving between opposite faces of rectangular slabs of the material. Physical situations of interest often display, of course, more complex geometries. In the case of lightning attachments or precipitation static, the current is injected into a series of points along the surface and then distributes itself (via a relaxation process) through the three-dimensional aircraft fuselage. Although detailed modeling of the process is difficult, it is clear that the above description will hold qualitatively. There will be differences in various formulas as a result of the geometric complexity but the basic conclusion that fiber contact dominates the observed composite material conductivity will hold.

The introduction of advanced composite materials causes a large number of problems for individuals concerned with the electromagnetic compatibility and survivability of defense systems. A significant effort has already been expended to predict electromagnetic scattering and penetration for all metallic structures. The applicability of this research to advanced composite materials is not known. If fundamental physical changes in composites could be made so that their electrical properties more closely approach those of metals, existing scattering and penetration algorithms could be applied to composites with improved accuracy.

The models of this section indicate that this goal could be approached in one of two ways: either increase the conductivity of the fibers or increase the fiber contact. The second path is ruled out by mechanical requirements. The resistance of composites to microbuckling is primarily determined by the fiber contact. As fiber contact increases, resistance to microbuckling decreases and, in general, these materials are fabricated so as to minimize fiber contact. Attempts to increase conductivities by increasing fiber contact would lead to an unacceptable degradation in mechanical behavior.

This forces us to examine fiber conductivities more carefully and develop techniques for increasing the conductivities without an accompanying decrease in specific strengths. This implies that the basic mechanical strengths of the fibers must be unchanged and, at the same time, their densities should not increase. These requirements, in conjunction with processing difficulties, rule out plating the fibers with metallic sheaths.

The model used above to calculate  $\sigma_T$  is the simplest possible in that it involves two rectangular fibers with a rectangular neck between them. It is of interest to examine a more realistic model--the random fiber model. The transverse conductivity is to be calculated for current through a series of parallel planes. The rectangular fibers are distributed across each plane with a probability  $f$ , the macroscopic volume fraction of the fibers. For a sample composed of two such planes (Figure 3), the transverse conductivity is calculated under the assumption that the boundaries of the two layers are equipotentials.



RANDOM FIBER MODEL

FIGURE 3

At any lateral point  $X$ , there are four possibilities concerning the material in the  $z$  direction:

- i) both layers are fiber; probability  $f^2$ ,
- ii) the first layer is fiber, the second matrix; probability  $f(1-f)$
- iii) the first layer is matrix, the second fiber; probability  $(1-f)f$ ,
- iv) both layers are matrix; probability  $(1-f)^2$ .

The total current flow is the sum of the currents associated with each of the four cases. For case i,

$$J_1 = \sigma_1 E = \sigma_1 (\Delta\phi/t)$$

because the electric field is uniform through the two layers and has a value  $\Delta\phi/t$  where  $\Delta\phi$  is the total potential drop and  $t/2$  is the thickness of a single layer. (Figure 3.)

In type ii situations, the electric field in the fiber,  $E_1$ , and in the matrix,  $E_2$ , are determined from the conservation of current density.

$$J_1 = \sigma_1 E_1 = J_2 = \sigma_2 E_2$$

and the recognition that the total potential drop across the two layers is  $\Delta\phi$ ,

$$E_1(t/2) + E_2(t/2) = \Delta\phi$$

Solving these latter two equations simultaneously yields

$$E_1 = 2 \left( \frac{\sigma_2}{\sigma_1 + \sigma_2} \right) \frac{\Delta\phi}{t}$$

The associated current density is

$$J_{1i} = \sigma_1 E_1 = 2 \left( \frac{\sigma_1 \sigma_2}{\sigma_1 + \sigma_2} \right) \frac{\Delta\phi}{t}$$

Similarly, for the other two cases,

$$J_{iii} = 2 \left( \frac{\sigma_1 \sigma_2}{\sigma_1 + \sigma_2} \right) (\Delta\phi/t)$$

$$J_{iv} = \sigma_2 (\Delta\phi/t)$$

The total current density is found by weighting each of the four individual probabilities and summing

$$J = f^2 J_1 + f(1-f) J_{1i} + (1-f)f J_{iii} + (1-f)^2 J_{iv}$$

Recognizing that  $J = \sigma_T E$  and  $E = \Delta\phi/t$  yields

$$\sigma_T = \sigma_1 f^2 + 4 \left( \frac{\sigma_1 \sigma_2}{\sigma_1 + \sigma_2} \right) f(1-f) + \sigma_2 (1-f)^2$$

For  $\sigma_1 \gg \sigma_2$  (the situation with graphite/resin composites), this reduces to

$$\sigma_T = \sigma_1 f^2 + 4\sigma_2 f(1-f) + \sigma_2 (1-f)^2$$

As long as  $f$  doesn't approach zero, it may be further concluded that

$$\sigma_T = \sigma_1 f^2$$

In graphite/epoxy samples with  $f = 0.6$ , direct measurement indicates that

$$\sigma_T = 200 \text{ mhos/meter and } \sigma_1 = 2(10^4) \text{ mhos/meter}$$

while the above equation predicts that  $\sigma_T = 7200$  mhos/meter.

If the basic random plane model is extended from two to three layers, the method of analysis remains the same but the algebraic complexity increases. Again, for  $\sigma_1 \gg \sigma_2$  and  $f$  not near zero, the transverse conductivity may be written as

$$\sigma_T = f^3 \sigma_1$$

Extending this reasoning produces the following table

Number of Layers in Model	$\sigma_T/\sigma_1$	$\sigma_T$ (mhos/m.)
1	$f$	$1.2(10^4)$
2	$f^2$	$7.2(10^3)$
3	$f^3$	$4.3(10^3)$
.	.	.
.	.	.
.	.	.
9	$f^9$	$2.0(10^2)$
10	$f^{10}$	$1.2(10^2)$
11	$f^{11}$	$7.3(10)$

The above values for  $\sigma_T$  were calculated using  $f=0.6$  and  $\sigma_1 = 2(10^4)$  mhos/m.

For a single ply of graphite/epoxy, the nominal thickness is 0.005 inches while the fibers have diameters of 0.0003 inches. This implies that the random plane model should contain approximately 17 layers ( $.005/.0003 = 16.67$ ). However, the leading term converges to the experimental value for only ten layers. However, with  $f=0.75$ , the random plane model yields a value of  $\sigma_T$  close to the experimental value with the number of planes equal to 17.

This strong dependence upon the number of planes in the model results from the use of only the leading term in the full expression for  $\sigma_T$ . As the number of planes increases, the calculation of terms other than the leading term becomes quite complex because one has to count all possible fiber-to-fiber paths through the sample.

A FORTRAN program has been written to count such paths but it is not, at present, operating correctly. The algorithm does not find all paths and

results in incorrect values of conductivity. The program details are not included in this report and this aspect of the research is continuing.

Although the models examined in this section have been simple, they lead to an important conclusion. The intrinsic conductivity of graphite/resin and boron/resin advanced composite materials can be increased by increasing the fiber conductivities.

### 3) ELEMENTS OF MICROSCOPIC FIBER CONDUCTIVITY AND IMPURITY DIFFUSION

Given the desirable goal of increasing fiber conductivity, it is necessary to observe two implicit constraints. If the enhanced conductivity fibers are to be useful in advanced composite materials, it is necessary that any process used to increase fiber conductivity must not decrease the specific strengths of the fibers to any significant degree.

To gain insight into possible methods for attaining these goals, the equations for the conductivity  $\sigma$  of a semiconductor provide a starting point.

$$\sigma = q(\mu_e n + \mu_h p)$$

where

$$q = 1.6(10^{-19}) \text{ coulombs,}$$

$\mu_e$ ,  $\mu_h$  are the electron, hole mobilities and

$n$ ,  $p$  are the densities of "free" electrons,  
holes per unit volume.

In the case of a metal, the hole concentration is, of course, zero.

The electron and hole mobilities essentially measure the ease with which charged particles move through the material under the influence of an external electric field. The mobilities depend primarily upon the atomic species of which the solid is composed as well as the crystalline perfection. In general, a higher degree of crystalline order implies a larger value of mobility.

These remarks lead to the observation that the conductivities of the graphite and boron fibers used in advanced composites could be increased by more careful attention to the processes whereby the fibers are formed (graphitization of a hydrocarbon and chemical deposition of boron on tungsten) to insure a higher degree of crystalline order. Such efforts have not been, to our knowledge, made.

Increases in electron and hole densities can result in large increases in conductivities and orders of magnitude increases result from relatively small additions of the proper impurity atoms. In a typical semiconductor, an addition of 0.1 parts per million of a donor impurity increases the conductivity by over five orders of magnitude.<sup>17</sup>

Although future confirming experiments will be necessary, it seems likely that such a small impurity addition to the fibers will not have a major effect upon either the mechanical strength or the mass density.

This process of adding small amounts of electrically active impurity atoms (either donors or acceptors) to semiconductors is known as "doping." It is widely used in fabricating solid state devices in silicon, germanium and compound semiconductors.

The next germane question is "Are graphite and boron fibers semiconductors?". Available evidence indicates that both materials are semiconductors in their normal composite forms. Semiconductor behavior has been observed in polycrystalline specimens of both graphite<sup>8</sup> and boron<sup>9</sup>.

One caveat is essential at this point. As impurity atoms are introduced into a host solid, their degree of electrical activity depends upon the crystalline perfection of the host medium. Given the high degree of atomic disorder present in the fibers used in advanced composite materials, it is highly probable that the doping process will not be as efficient as it is in single crystal silicon. This inefficiency will lead to limits upon the amounts of conductivity enhancement attainable in both graphite and boron fibers.

The most natural method of adding impurities to fibers utilizes the thermal diffusion of impurity atoms under the influence of a concentration gradient. Before describing the experimental aspects of impurity diffusion, the basic elements of linear diffusion theory will be reviewed.

The first order theory assumes that the impurity atom flux  $\bar{J}$  (atoms/cm<sup>2</sup>-sec) is linearly related to the spatial gradient of the impurity concentration  $N$  (atoms/cm<sup>3</sup>). The relationship between  $J$  and  $N$  is called Fick's First Law<sup>10</sup> and is written

$$\bar{J} = -D\bar{\nabla}N$$

where  $D$  is the diffusion coefficient (cm<sup>2</sup>/sec) and  $\bar{\nabla}$  the spatial gradient operator. The diffusion coefficient's numerical value is usually obtained from experiment.

Invoking the conservation of impurity atoms results in Fick's Second Law<sup>11</sup> which may be written as

$$\frac{\partial N}{\partial t} = \bar{\nabla} \cdot D\bar{\nabla}N$$

where  $t$  is the time.

The problem of interest involves the diffusion of impurity atoms into fibers. For analytical ease, the fibers are modeled as being infinitely long so that end effects may be neglected and the fibers are also assumed to have circular cross-sectional areas. Given that the source of impurity atoms is

uniformly distributed either on or near the fiber surface, it follows that the distribution of the diffused impurity species ( $N(r,t)$ ) will be independent of the polar angle. The impurity concentration depends only upon the radial distance,  $r$  and the time,  $t$ . In this case, Fick's Second Law takes the form

$$\frac{\partial N}{\partial t} = \frac{1}{r} \frac{\partial}{\partial r} r D \frac{\partial N}{\partial r}.$$

If the initial distribution of impurities in the fiber is known and the source used to add impurities to the fibers during diffusion is suitably characterized, solutions to this partial differential equation will predict the resultant impurity profile for a diffusion at a given temperature  $T$  and time  $t$ . The coefficient  $D$  is a measure of the relative ease with which impurity atoms move through the host material. The larger the value of  $D$ , the faster the impurity atoms diffuse. Although diffusion theoretically occurs in any physical system in which a non-zero spatial gradient of impurity concentration exists, the diffusion mechanism is so slow at room temperature in solids as to be negligible. As a consequence, any intentional diffusion processing is carried out at elevated temperatures. A suitable range of temperatures for a given system may be predicted from a knowledge of the diffusion coefficient  $D$ .

A solution to Fick's Second Law has been found<sup>11</sup> in closed-form for the situation in which a cylinder of radius  $R$  is initially impurity free and exposed to a constant surface impurity concentration during an elevated temperature diffusion cycle for a time  $t$ . It is assumed that the diffusion coefficient  $D$  is a constant. The solution is

$$N(r,t) = N_0 \left[ 1 - \frac{2}{R} \sum_{n=1}^{\infty} e^{-\alpha_n^2 t} \left( \frac{J_0(r\alpha_n)}{J_1(R\alpha_n)} \right) \right]$$

where  $J_0$  is the Bessel function of the first kind of order zero,

$J_1$  the Bessel function of the first order and

$\alpha_n$  are the roots of  $J_0(R\alpha_n) = 0$ .

Numerical evaluation<sup>11</sup> of this formula reveals that

$$N(0,t_0) = N(R,t_0) = N_0 \text{ to within 1\% for}$$

$$D t_0 = R^2.$$

Although little information could be found regarding the diffusion coefficients of impurities of interest in graphite and boron, estimates of the time required to produce a uniform impurity distribution may be made using

values of  $D$  for electrically active impurities in silicon. For example,  $D = 10^{-12}$  cm<sup>2</sup>/sec. for phosphorous diffusing in silicon at 1200° C. The time  $t_0$  required to produce a nearly uniform impurity concentration is

$$t_0 = R^2/D = 10^{12} R^2$$

For graphite fibers,

$$R \approx 3(10^{-4}) \text{ cm}$$

and  $t_0 \approx 9(10^4) \text{ sec} = 25 \text{ hours}$

This time may be reduced significantly by increasing the temperature at which the impurities are diffused since  $D$  has an exponential dependence on the temperature  $T$ , i.e.,

$$D(T) = D_0 \exp(-Q/T) \quad (D_0, Q \text{ constants})$$

In summary, thermal diffusion is a process whereby impurity atoms move into a solid under the influence of an impurity concentration gradient. There is, on the average, a net flux of impurity atoms from regions of high concentration to regions of low concentration. This aggregate motion is a consequence of the random walk motion of the impurity atoms. This process is well characterized theoretically and has been widely used experimentally to introduce impurities into semiconductors. For these reasons, high temperature diffusion has been chosen as the method to add selected impurities to graphite and boron fibers.

It is evident from the discussion of this section that little quantitative information is, at present, available concerning impurity diffusion in graphite and boron. Most importantly, numerical values for the diffusion coefficients as a function of temperature for various impurities in graphite and boron are not known. The experimental work described in the following sections contains no quantitative analysis of the impurity distributions resulting from the diffusion cycles. The experiments were intended to assess, in a preliminary way, the feasibility of modifying fiber conductivities via impurity diffusion. In follow-on work, secondary ion mass spectroscopy will be used to obtain detailed impurity profiles resulting from specific temperature-time diffusion cycles and, from this information, specific numerical values for diffusion coefficients will be derived. Such detailed information was not a goal of this year's research activities.

In the next sections, the physical and electrical properties of as-grown fibers are examined. In addition, techniques used to make repeatable, electrical contacts to both graphite and boron fibers are discussed in detail.

#### 4) GRAPHITE FIBERS

There has been a significant amount of research conducted concerning the response of graphite/epoxy composites to laboratory simulations of electromagnetic excitations<sup>2,13,14</sup>. Such material behavior must be thoroughly understood before aircraft made primarily of composite materials can be safely designed and flown. The research to date has been empirical and has resulted in the conclusion that protective metal thin films or mesh are necessary to prevent severe structural degradation from lightning attachment. Some contrary opinions<sup>15</sup> have also been expressed.

A complete model of graphite/epoxy response to electromagnetic excitation involves several complex elements. Pre-requisites include a knowledge of the low-level (linear) response, current-voltage characteristics of the graphite fibers, the high-level (non-linear) response, a statistical knowledge of fiber arrangements and some description of fiber-to-fiber contact, solutions detailing the distribution of currents in fiber/epoxy structures and a thermal transient analysis of such systems. The first task is to examine the electrical responses of the fibers. The low frequency conductivity of unidirectional graphite/epoxy composites has been reported<sup>4</sup> and the need for careful sample preparation and standardization has been discussed.<sup>15</sup> In this section, we examine the linear current-voltage characteristics of graphite fibers as well as the threshold electric fields and current densities associated with failure.

Preliminary investigation revealed that fibers produced by various companies had different conductivities. To simplify the following discussions, the work reported involved only one fiber type--Thornel T300 as used in Narmco 5208 pre-preg tapes.

Individual graphite fibers have radii on the order of a few micrometers and are difficult to handle. In general, it was convenient to immerse a segment of graphite tow in methanol and use teflon coated tweezers to separate individual fibers from the bundle. Microscopic observation and a steady hand during this procedure improved the success rate. The fibers, in lengths from two to four centimeters, were mounted on pre-cleaned glass microscope slides. This was accomplished by applying electrically conductive silver paint to the ends of the fibers. When dry, this paint holds the fiber to the glass slide and provides an ohmic electrical contact.

Other research<sup>7</sup> indicates that the conductivity of graphite/epoxy composite materials is independent of frequency from DC to 50 MHz. Because the electrical behavior of composites is governed by the electrical conductivity of the fibers, electrical examination of the fibers at DC using a voltage source-voltmeter-ammeter combination or at 400 Hz using a standard curve tracer provided sufficient information. The fiber conductance,  $G$ , for low-level excitation is simply the ratio of the current  $I$  to the voltage,  $V$ . With this ratio, the conductivity  $\sigma$  for current flow along the fiber axis may be calculated from a knowledge of fiber length  $L$  and cross-sectional area  $A$ .

$$G = \frac{I}{V} = \frac{\sigma A}{L}$$

To further characterize the fibers physically, both optical and scanning electron micrographs of the individual fibers were made. Some fibers, as received, were partially covered with a white ash-like substance but this was readily removed when the fibers were immersed in methanol.

All measurements were taken with the fibers in room atmosphere with a temperature of 20°C and a relative humidity on the order of 60%. In some situations, it was useful to vary the temperature of the fibers and this was accomplished by means of a resistance heated air gun.

The fibers measured had an average DC conductivity of 20,000 mhos/m with a range of 14,000 to 30,000 mhos/m. All of the fibers displayed linear electrical responses up to maximum electric fields of approximately 4000 volts/m. Thirty percent of the samples broke at electric fields below this value.

In some geographic configurations graphite/epoxy composites display non-linear electrical characteristics at much lower values of electric field. To further understand the difference between the bare fibers and the graphite/epoxy, a number of graphite fibers were coated with epoxy. These fibers had lower threshold power densities. If the ambient temperatures were increased via heat gun, the epoxy coated fibers would break at excitation levels at which they were stable at room temperature. In one case, the electric field across the sample was held at 3500 volts/m and the current remained constant. Upon application of the external heat, the current increased and the fiber failed. The current increase observed would seem to rule out the force of the heat gun's air stream as the cause of fiber breaking.

The detailed electric field and current density thresholds associated with breakdown are shown in Table I below.

Breakdown Thresholds		
	E(volts/m)	J(amp/m <sup>2</sup> )
minimum	3.2(10 <sup>3</sup> )	57.6(10 <sup>6</sup> )
average	3.7(10 <sup>3</sup> )	103.2(10 <sup>6</sup> )
maximum	4.4(10 <sup>3</sup> )	125.1(10 <sup>6</sup> )

TABLE I

These results indicate that thermal mechanisms are involved in the failure of the graphite fibers. However, the modeling required to analyze the situation is complex. The energy generated in the fiber via resistive heating will be, in steady state, balanced by three processes: heat conduction into the glass slide, heat convection into the air and radiation. No models for conductive heat flow from a cylinder into a rectangular glass plate could be found with the desired attributes of accuracy and computational simplicity. As mentioned above, no visible color changes in the fiber were observed which would have indicated increases in temperature as large as 1000°C. For this reason, it is likely that local temperatures increase at points along the

fiber, possibly due to the presence of local constrictions in the fiber cross-sectional area. These defects give rise to locally enhanced temperatures and the resultant incandescent failure which we observed.

Figure 4 illustrates a simple model in which a local defect of length  $\delta$  decreases the area from  $A$  to  $A'$ . The DC current must be constant along the fiber,

$$J'A' = JA, \quad E' = J'/\sigma, \quad E = J/\sigma,$$

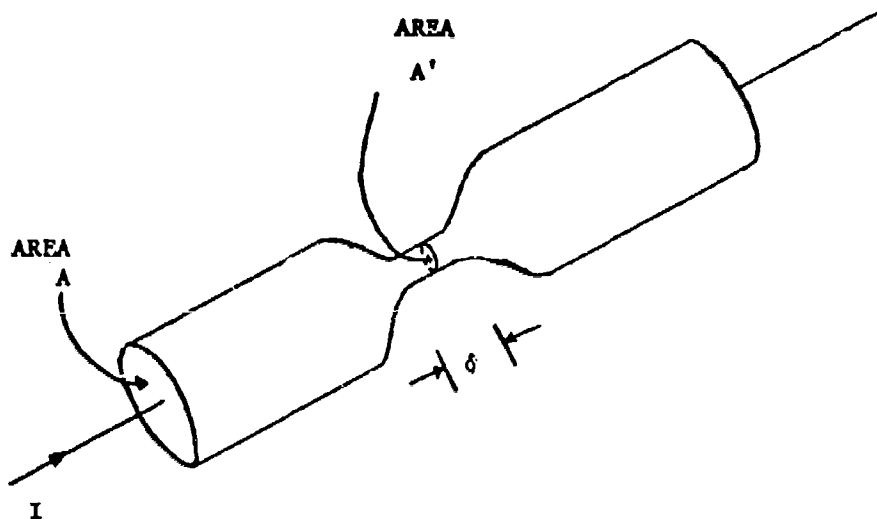
where primed quantities denote those in the constricted area.

$$\text{Define } \eta = A/A', \quad J' = \eta J, \quad E' = \eta E$$

The power density  $P$  is the produce of current density and electric field.

$$P' = \eta^2 P$$

A 30% reduction in area will result in a doubling of the local power density. This naturally produces a rise in fiber temperature with an accompanying increase in the probability of fiber failure as a result of oxidation.



CURRENT CONSTRUCTION MODEL

FIGURE 4

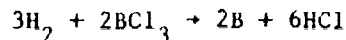
Scanning electron microscopy revealed significant surface defects but it was not possible to determine the restriction in areas associated with the defect structure. Numerical estimates of the local heating of the fibers cannot be made without this information.

The relationship between this mechanism and lightning degradation is clear although quite difficult to model analytically. When a large current is injected into a graphite/epoxy composite, the several orders of magnitude difference between the conductivities of the graphite and the epoxy result in the total current being confined to the fibers. In the vicinity of the attachment point, these currents will certainly exceed the threshold currents for fiber failure. As fibers break, the current is forced into other fibers and more breakage occurs. Associated with this is epoxy softening and mechanical failure.

In summary, although individual graphite fibers are difficult to separate from tows and handle, they are easily characterized electrically. Their current-voltage characteristics are linear until the fibers break and the fibers have an average conductivity of  $2(10^4)$  mhos/meter.

#### 5) BORON FIBERS

Boron fibers were supplied by Avco in three different diameters: 4, 5.6 and 8 mils (0.01, 0.14 and 0.02 cm). These fibers are produced by chemically depositing boron on a heated tungsten wire of 0.0018 cm. diameter in an atmosphere of  $H_2 + BCl_3$ . A reduction reaction occurs.

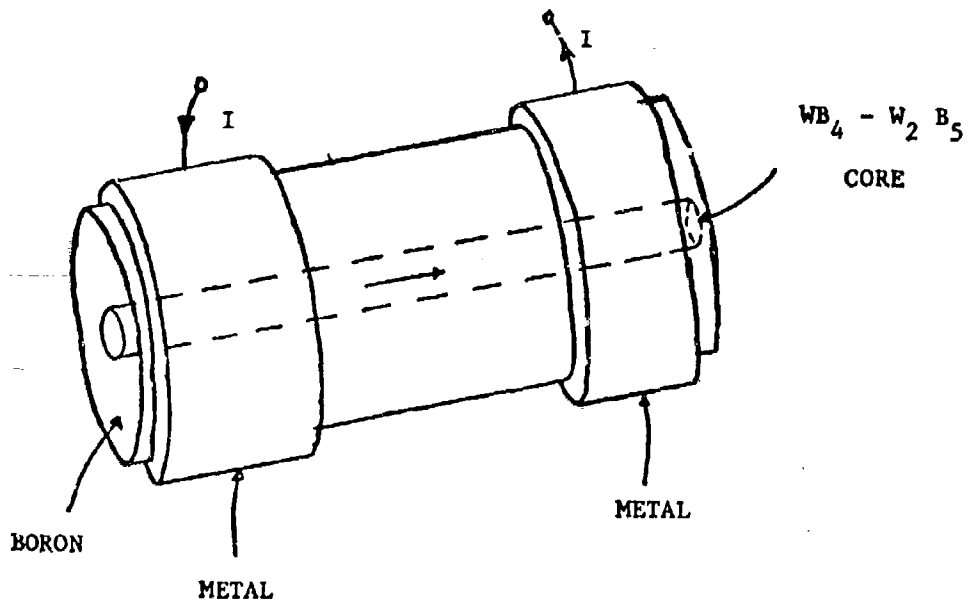


The boron is deposited on the heated tungsten wire and complete reaction of the tungsten occurs. The remaining core consists of a mixture of  $WB_4$  and  $W_2B_5$ . The core diameter is unchanged and is essentially coated with pure boron.<sup>17</sup>

All of the processing details (exact temperature, gas concentrations and flow rates) are proprietary and are not available.

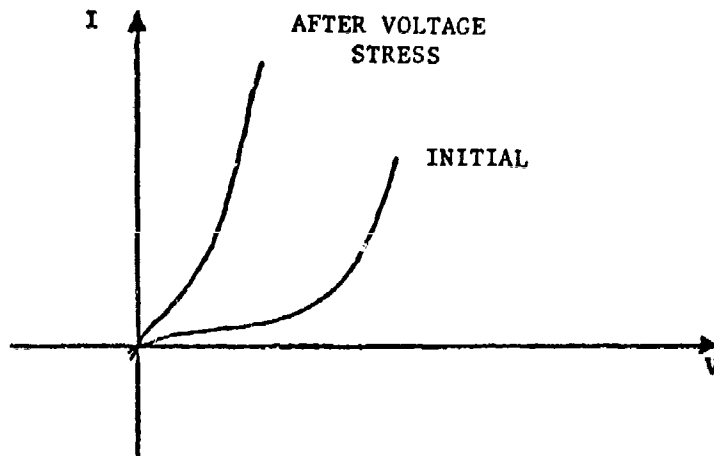
In order to characterize the as-grown fibers electrically, it was necessary to make ohmic electrical contact and this proved to be challenging. A procedure identical to that used for graphite was tried initially. Boron fibers were cleaned via ultrasonic agitation in trichlorethylene and rinsed in acetone and methanol. The fibers were dried in prepurified nitrogen and mounted on microscope slides using a conductive silver ink. Care was taken to insure the isolation of the fiber ends so as to force current to flow through the boron sheath radially inward as shown in Figure 5. The resultant current-voltage characteristics are sketched in Figure 6. Not only are they non-linear but they display memory.

It was evident that these results could not be used to calculate an intrinsic conductivity of the boron fibers. Variations of the cleaning procedure



CONTACT GEOMETRY

FIGURE 5



$I$ - $V$  CHARACTERISTICS OF BORON FIBERS WITH INDIUM CONTACTS

FIGURE 6

were tried in attempts to etch any contaminated surfaces which could have been responsible for non-linear effects. These treatments included etches in both nitric and sulfuric acid. The rectifying nature of the silver-boron interface and the non-linear current-voltage characteristics persisted although various acid concentrations and etching times were tried.

Contact formation was next attempted by "dipping" boron fibers into molten indium. Relatively pure indium (99.999%) was melted in a Pyrex beaker over a hot plate in an argon atmosphere. Cleaned boron fibers were dipped into the molten indium using a glove box. This procedure naturally resulted in the formation of contacts between the indium and the central tungsten boride core as well as the boron sheath. In situations in which electrical isolation was desired between the indium contact and the relatively conductive core, the ends of the fibers were cleaved using a straight edge razor blade and the indium caps removed. Figures 7 and 8 illustrate this procedure. It was during this cleaving process that a lack of good metallurgical contact between the indium and the boron was observable. In some cases, the entire indium contact would pull away from the fiber as the razor blade was cutting through.

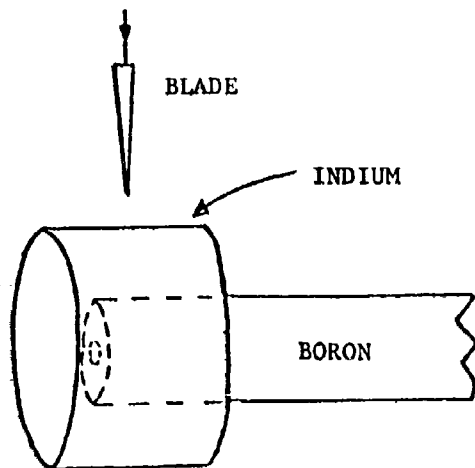
This lack of mechanical adhesion was troubling and, although some linear current-voltage characteristics were observed using this process, instabilities and hysteresis persisted. The measured current-voltage curves were not necessarily truly indicative of current through the fibers only. Rectifying effects were still in evidence and another contacting procedure was needed before a conductivity could be uniquely assigned to the chemically vapor deposited boron.

The phase diagrams for boron and various metals were next examined. Although it is difficult to generalize about the complex subject of metal-semiconductor contacts, it is generally found that the probability of fabricating an ohmic contact between a given semiconductor and a given metal increases as does the number of low temperature phases formed between the two constituents.

The various phase diagrams revealed relatively few candidates among the easily deposited metals. Nickel was chosen because it is easily electroplated and forms compounds with boron at temperatures above 1000°C. The detailed procedures used for fiber cleaning and nickel electroplating are given in Appendix A.

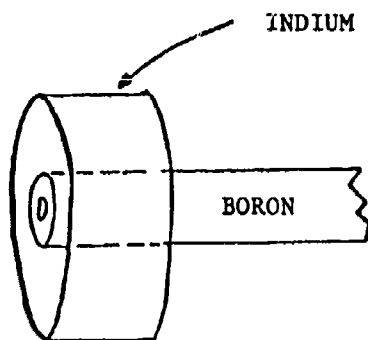
The nickel-boron contacts proved quite satisfactory from both mechanical and electrical viewpoints. Although formal tests of the mechanical adhesion of the electroplated nickel to the boron were not conducted, no separation during routine laboratory handling of the fibers were observed. In addition, the current-voltage characteristics of the boron fibers, with and without electrical isolation of the tungsten boride core, have been linear.

The geometry used in the i-v measurements is shown in Figure 9. In order to relate the measured conductance to the boron conductivity, the conductive core was isolated from the nickel plating using a suitable wax (Appendix A). To model current flow in the fibers, it is assumed initially that the core



INDIUM CONTACT TO FIBER CORE

FIGURE 7



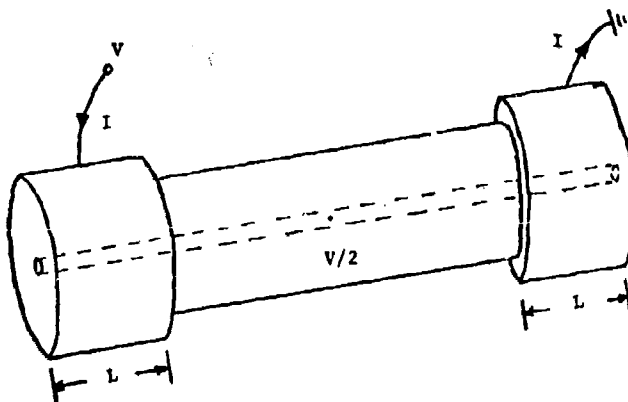
INDIUM ISOLATED FROM CORE

FIGURE 8

conductance is large compared to that associated with the boron and voltage drops along the boride core are neglected. Further, the contacts are circularly symmetric and this implies a circularly symmetric electrostatic potential. For the geometry shown in Figure 9, we write the static potential as

$$\phi(r) = B \ln(a/r)$$

where  $a$  is the radius of the boride core,  
 $R$  the outer radius of the boron sheath and  
 $B$  is a constant fixed by the boundary conditions.



GEOMETRY FOR CALCULATION OF  $\sigma_B$

FIGURE 9

By symmetry, a voltage drop of  $V/2$  will appear across each nickel coated boron segment when a voltage of  $V$  is applied across the entire fiber. Using this fact, the constant  $B$  in the above equation can be evaluated. The total potential takes the form.

$$\phi(r) = \frac{V}{2} \frac{\ln(a/r)}{\ln(a/R)}$$

From this, it is straightforward to calculate the electric field and the current density and finally the total current  $I$ .

$$I = -2\pi r L J = \frac{\pi \sigma V L}{-\ln(a/R)} \quad \text{or} \quad \sigma = \left(\frac{I}{V}\right) \left(\frac{\ln(R/a)}{\pi L}\right)$$

(the minus sign is needed on the left since positive  $J$  implies current flowing out)

The first measurements were made on samples with 8 mils diameter and yielded the following results.

Sample Number	V(volts)	I(amps)	$\sigma$ (mhos/m)
AA 6	0.5	$.54(10^{-3})$	.0837
AA 7	1.0	$1.05(10^{-3})$	.0814
AA 8	1.0	$1.05(10^{-3})$	.0814

(for all samples,  $L = 1$  cm.).

In all cases, the current-voltage curve was linear for both polarities of applied voltage and displayed no evidence of any rectifying behavior at the nickel-boron interface. In addition, the calculated values of conductivity are consistent from fiber-to-fiber.

Subsequent measurement of a total of seven samples taken from the same spool of fiber yielded essentially identical current-voltage curves and resulted in an average boron conductivity of

$$\bar{\sigma} = 0.093 \text{ mhos/m.}$$

Next, four fibers of 5.6 mil diameter were nickel plated and the conductivity calculated using the model developed above. The results of this analysis were

Sample Number	(mhos/m)
BB 1	0.1
BB 2	0.155
BB 3	0.097
BB 4	0.1

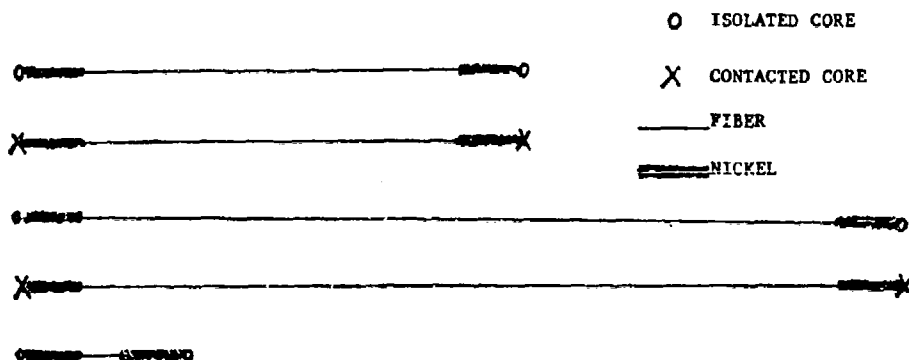
$$\bar{\sigma} = 0.113 \text{ mhos/m.}$$

Although there is more scatter in these values than the corresponding 8 mil diameter fiber values, the cluster is good and yields a comparable value for the average conductivity of the boron sheath. It is likely that thickness variations in the boron sheath are greater in 5.6 mil fibers than in 8.0 mil fibers and produce larger conductance scatter.

The above set of experiments provided initial electrical characterization of the "as-grown" boron fibers. In order to more fully understand the mechanism of current flow in these fibers, a series of electrical measurements were made on fibers in which nickel contacts were plated directly to the tungsten boride core as well as the boron sheath. The fibers were 5.6 mils in diameter and typical results are shown in the following table.

Sample	Length (cm)	Plated length (each end) (cm)	Direct Contact to Core?	DC Resistance (ohms)
1	9.0	1.0	No	800
2	9.0	1.0	Yes	300
3	16.0	1.0	No	1120
4	16.0	1.0	Yes	500
5	2.8	1.0	No	714

These five samples are sketched in Figure 10.



SAMPLE GEOMETRIES

FIGURE 10

It is assumed that the core is homogeneous with respect to fiber length and the core is characterized by a resistance per unit length,  $r_c$  (ohms/cm). When this value is determined, the electrical conductivity of the core will be fixed because the core area is known. The symbol  $R_B$  is used to denote the resistance of a nickel coated boron cylinder of length 1 cm. This is the resistance associated with a radial current from the nickel to the conductive core. In terms of these symbols, expressions for the resistances of each of these five samples may be written.

The factor of 2 before  $R_B$  is a reflection of the existence of two radial paths through the boron sheath in each sample.

Sample	Expression for Resistance
1	$8r_c + 2R_B$
2	$9r_c$
3	$15r_c + 2R_B$
4	$16r_c$
5	$1.8r_c + 2R_B$

The algorithm used to write these equations should be clear. The quantity  $R_B$  does not appear in the expressions for Samples 2 and 4 because the resistance of the boron sheath is shorted by the direct contact between the nickel and the core. Electrical isolation in Samples 1, 3 and 5 was provided by masking the ends of the boron fibers with a non-conductive wax prior to the electroplating.

Using these five expressions and the measured values of resistance, values for  $r_c$  and  $R_B$  can be obtained. The measured values of resistance for Samples 2 and 4 lead directly to

$$2 \text{ (9 cm.)} \quad r_c = 33.3 \text{ ohms/cm}$$

$$4 \text{ (16 cm)} \quad r_c = 31.3 \text{ ohms/cm}$$

The average value of the core resistance obtained for all of the samples measured during the research period was 32 ohms/cm. Using this average value, the quantity  $R_B$  may be calculated using the experimental results from Samples 1, 3 and 5.

$$1 \text{ (9 cm.)} \quad R_B = \frac{800 - (8)(32)}{2} = 272 \text{ ohms}$$

$$3 \text{ (16 cm.)} \quad R_B = \frac{1120 - (15)(32)}{2} = 320 \text{ ohms}$$

$$5 \text{ (2.8 cm.)} \quad R_B = \frac{714 - (1.8)(32)}{2} = 328 \text{ ohms.}$$

There are, of course, variations in this value caused by differences in the "as grown" fibers as well as uncontrollable variations in the total length of the plated electrodes. The averaging of all available data yields a value of 300 ohms for  $R_B$ .

This result allows a more accurate calculation of the boron conductivity than was possible in the last section in which the resistance of the tungsten boride core was assumed to be zero. The value obtained is

$$\sigma_B = .25 \text{ mhos/m.}$$

This value is two to three orders of magnitude greater than that reported by other investigators for pure, single crystal boron. This discrepancy is not alarming in view of the large differences between the fibers and the materials used by other investigators. In particular, the boron of which the fibers are made is polycrystalline and the impurity content is simply not known. As mentioned above, the details of growth are proprietary information. Because boron is a semiconductor, the presence of relatively small amounts of impurities would account for a large change in conductivity as discussed in Section 3 of this report.

For a fiber of 0.01 cm. diameter, it is possible to define an effective conductivity for current along the fiber. The fiber conductance  $G$  is written

$$G = \frac{\sigma_{\text{eff}} A}{L}$$

where  $A$  is the fiber area and  $L$  the length. But this conductance is the sum of the conductances of the core and the boron sheath.

$$\begin{aligned} G &= G_c + G_B \\ &= \frac{\sigma_c A_c}{L} + \frac{\sigma_B A_B}{L} \end{aligned}$$

where the subscript  $c$  denotes core quantities and  $B$  implies boron sheath quantities.

The effective fiber conductivity can be written as

$$\sigma_{\text{eff}} = \sigma_c (A_c/A) + \sigma_B (A_B/A).$$

All three areas and  $\sigma_B$  are known. The core conductivity can be readily calculated from the known value of resistance/length, i.e.,

$$r_c = 1/\sigma_c A_c \quad \text{or} \quad \sigma_c = 1/r_c A_c.$$

The core diameter is 0.0018 cm,  $r_c = 32$  ohms/cm and the core conductivity is calculated as

$$\sigma_c = 3 (10^5) \text{ mhos/m.}$$

The effective fiber conductivity is then determined.

$$\sigma_{\text{eff}} = 2.3 (10^3) \text{ mhos/m.}$$

Essentially all of the current is confined to the highly conductive core.

The above information concerning the electrical conductivity of graphite and boron fibers was gathered at room temperature, 300<sup>o</sup>K. It is of interest to investigate the temperature dependence of the conductivity because this behavior provides information as to the relative amounts of impurities present in a given semiconductor sample. It is well known in semiconductor device physics that such materials display a conductivity versus temperature curve<sup>17</sup> similar to that shown in Figure 11. It is important to recognize that the logarithm of the conductivity is plotted versus the reciprocal of the absolute temperature T. This means, of course, that temperature increases as one moves from right to left along the horizontal axis.

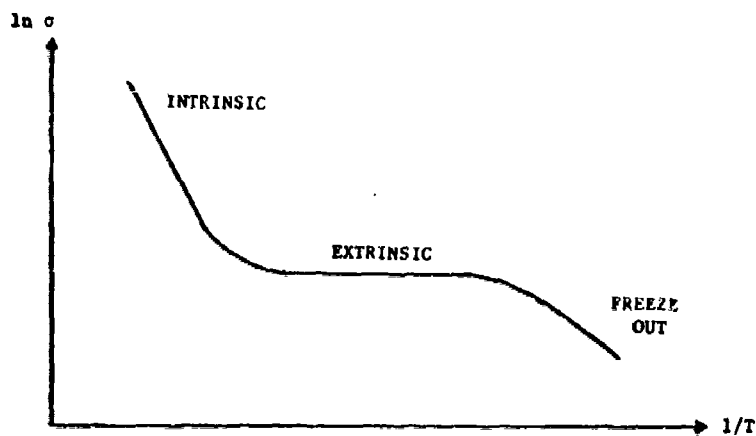
There are three distinct regions associated with this curve. The first, occurring at high temperatures, is termed the intrinsic region and the conductivity displays an exponential dependence on the reciprocal of temperature. Although the theoretical details are not of interest here, the physical reason for this behavior is simply that the thermally generated electrons and holes increase in number as the temperature increases and finally attain such large values that they swamp out any effects associated with electrically active impurities. All semiconductors will eventually attain this intrinsic behavior as their temperature is increased.

The second segment, the so-called extrinsic region, is one in which the thermally generated holes and electrons are insignificant in number in comparison with those associated with donors and/or acceptors. In this region, changes in temperature still affect the thermally generated carriers but, since they are present in negligible quantities, this has no effect on the sample conductivity. Finally, at very low temperatures, a third regime becomes apparent in which the conductivity decreases with decreasing temperature because the electrical effects of the donors and the acceptors are vanishing as the electrons and holes associated with these impurities "freeze" back onto their parent impurity atoms. This process normally begins at temperatures in the vicinity of 100<sup>o</sup>K and is not considered significant in our temperature investigations.

No detailed studies of conductivity variations with temperature were performed but a series of preliminary measurements were made using 0.02 cm. diameter boron fibers. The plated nickel contacts were isolated from the sample ends and, consequently, from the highly conductive boron tungstide core.

The fiber was mounted on a glass slide which was placed atop a large aluminum block on a hot plate. The block provided additional thermal mass and prevented rapid fluctuations in temperature as the hot plate heating elements cycled on and off. A chromel-alumel thermocouple was placed

adjacent to the boron fiber and the voltage developed across this junction when compared to a reference junction kept in an ice water bath was measured on a potentiometer.



CONDUCTIVITY-TEMPERATURE PROFILE

FIGURE 11

This fiber resistance  $R$  is shown as a function of the temperature  $T$  ( $^{\circ}\text{C}$ ) in Figure 12.

The sample resistance  $R$  may be written in terms of the resistivity  $\rho$  as

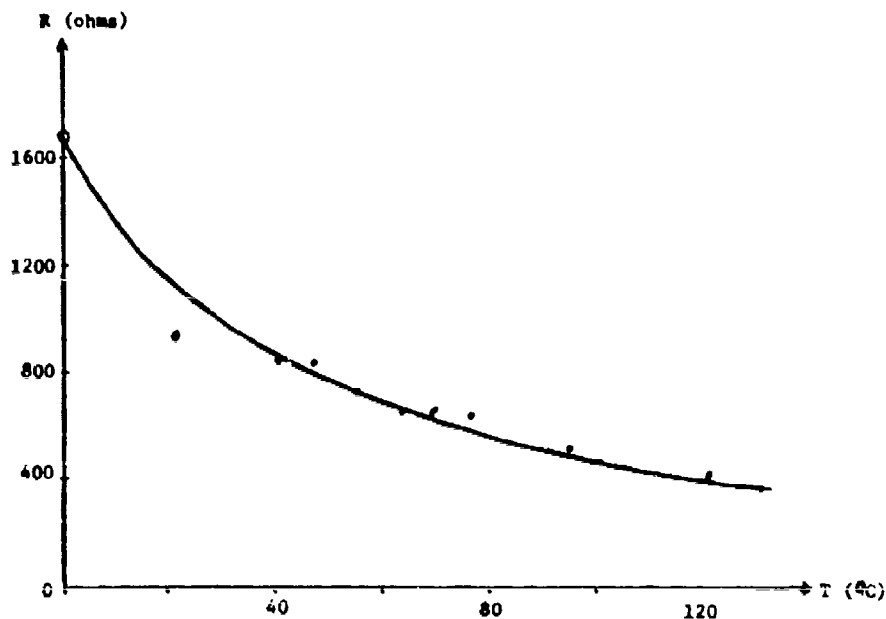
$$R = \gamma\rho$$

where  $\gamma$  is a constant determined by the details of the sample geometry. From this it follows that

$$\ln R = \ln \gamma + \ln \rho$$

and, neglecting thermal expansion effects,

$$\frac{\partial \ln R}{\partial (1/T)} = \frac{\partial \ln \rho}{\partial (1/T)} = - \frac{\partial \ln \sigma}{\partial (1/T)}$$



BORON FIBER R-T CURVE

FIGURE 12

Simple semiconductor theory<sup>17</sup> reveals that

$$\sigma = K e^{-E_g/2kT}$$

where  $K$  is effectively a constant,  $E_g$  the forbidden energy gap and  $k$  is Boltzmann's constant.

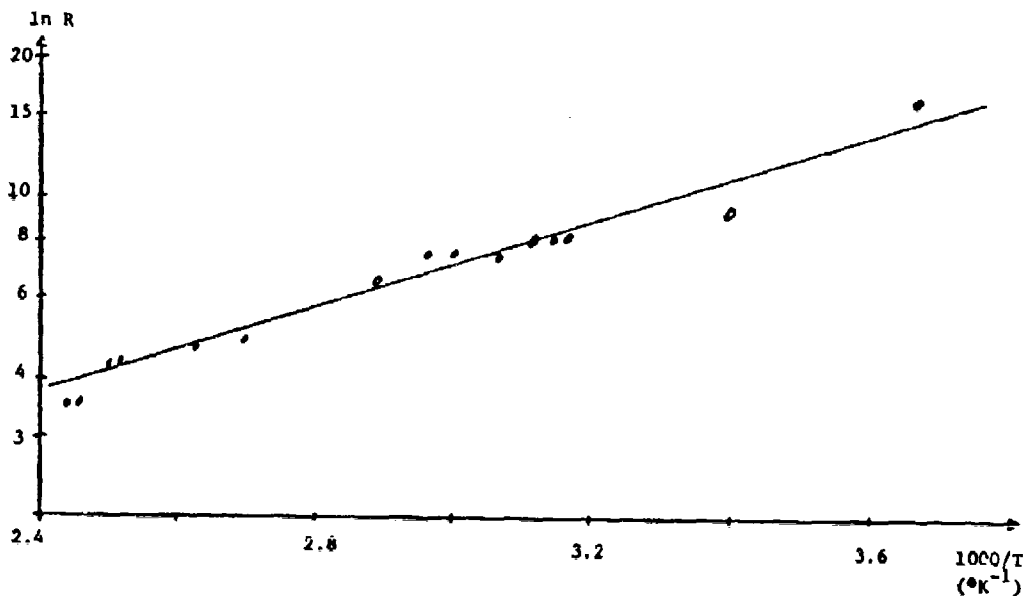
It follows that

$$\frac{\partial \ln \sigma}{\partial (1/T)} = -E_g/2k.$$

The slope of a plot of  $\ln R$  vs  $1/T$  is simply the negative of the forbidden energy gap divided by  $2k$ . The values of Figure 13 imply a value of

$$E_g = 0.19 \text{ eV}$$

The results reveal that the boron fibers are in the intrinsic range at room temperature and are characterized by a forbidden energy gap of 0.19 eV.



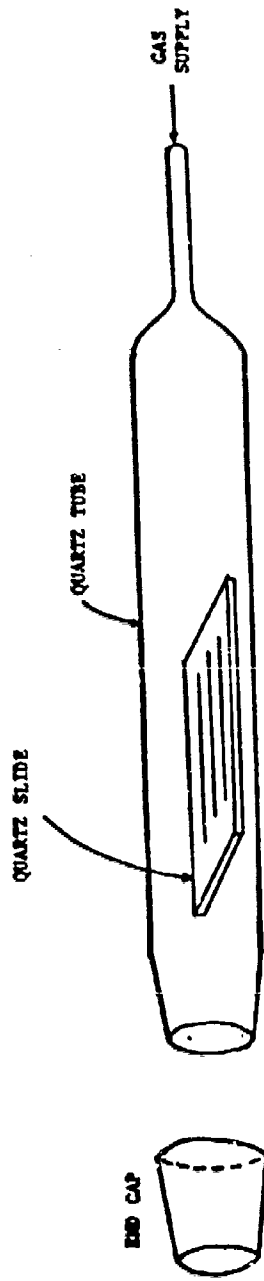
BORON FIBER ENERGY GAP

FIGURE 13

This completes the initial phase of the low frequency electrical characterization of graphite and boron fibers. The methods of contacting along with the derived values of conductivity for both fiber types provide a benchmark against which the results of various doping techniques can be evaluated. In the next section, the details of the diffusion experiments are presented.

## 6) DIFFUSION EXPERIMENTS

The basic equipment used to introduce impurities into both graphite and boron fibers was a simple diffusion furnace as sketched in Figure 14. It is composed of an open ended quartz tube which is embedded in thermal insulation and heated by adjacent carbon resistive heating elements. The elements are excited by 60 Hz currents and, when necessary, the amount of heating is controlled by a feedback system which uses as inputs the desired tube temperature and the actual tube temperature as measured by a thermocouple. In this simple furnace, the thermocouple is slid along the horizontal axis of the quartz tube through one of the open ends until it is in the zone in which the fibers will



BASIC DIFFUSION FURNACE

FIGURE 14

be placed. For our initial experiments, it was unnecessary to have precise temperature control and the feedback system was not used although the furnace temperature was constantly monitored using the thermocouple itself. Temperature fluctuations were controlled to  $\pm 50^{\circ}\text{C}$  manually.

One end of the quartz tube is connected to a fitting which allows the introduction of any gases desired. In this work, nitrogen and argon have both been used to provide inert furnace atmospheres. Since the purpose of the experiments is to examine the effects of intentionally introduced impurities, it is essential that no extraneous impurities be allowed access to the system. Both nitrogen and argon are chemically and electrically inert and serve this function adequately; although problems did arise in the case of nitrogen as will be discussed below, and the later experiments used argon exclusively.

The other end of the furnace is fitted with a removable quartz cap which provides access to the tube for the insertion of the fibers. The small size of the graphite fibers caused some difficulty and quartz slides, grooved to provide secure locations for the fibers, were used as convenient carriers.

As discussed in Section 3, the addition of suitable impurities to graphite and boron fibers is expected to increase the intrinsic electrical conductivity of these fibers via a semiconductor doping mechanism. It is important, at this point, to examine the possible atomic species which could be used as electrically active impurities. Both single crystal and polycrystalline boron are semiconductors and are composed of atoms from the third group of the Periodic Table. Applying standard semiconductor concepts, it is anticipated that impurities from the fourth column of the Periodic Table would act as donors while impurities from the second column would act as acceptors. Of the impurities in these two categories, carbon was selected as an easily obtainable species. Silicon and germanium could also be used but they have higher atomic masses and are likely to diffuse more slowly than carbon.

Graphite describes an allotropic form of carbon which occupies the fourth group of the Periodic Table and column five impurities should be donors while column three impurities should be acceptors. These impurities are widely used in preparing silicon integrated circuits and are easily available in a number of useful forms. Boron, phosphorous, gallium, indium, and aluminum are all possible candidates but only boron was used so as to reduce the number of experimental variables.

Having chosen the impurity species, a method was needed whereby they may be introduced into the fibers. Again, Section 3 discusses the process of thermal diffusion in general terms without specifying suitable ways of introducing impurities. There are two such processes in common use: the first involves introducing the impurities via the gas flow into the quartz diffusion tube while the second requires that the fibers be coated with a suitable compound containing the impurity species of interest. In both techniques, the goal is to insure a high concentration of the impurity species at the surface of the fiber. It was considered important that the impurities diffuse into the fibers with cylindrical symmetry so as to avoid any complications introduced by angular variations in the final impurity profile. For this reason, a method was selected by which the fibers could be uniformly coated using a

dipping procedure. In any situation in which the impurities were introduced in the gas stream, the surface of the fiber lying on the quartz flat would be shielded from the impurity atoms. This is not a fundamental objection because the fibers have small diameters and uniform impurity distributions would undoubtedly result from the second method if the diffusion times were sufficiently long and the diffusion temperatures were sufficiently high. There was, as mentioned above, no literature data to predict suitable times and temperatures and it was felt that the coating procedure would produce the most uniform results in this set of initial investigations.

All fibers were cleaned prior to coating and insertion into the diffusion furnace. The graphite fibers were cleaned by means of a three-step solvent sequence; they were first immersed in trichlorethylene, rinsed in acetone and methanol and dried under a heat lamp. The boron fibers were etched in hot sulfuric acid, rinsed in distilled water and methanol and dried in a purified nitrogen stream. No attempts at varying these cleaning procedures were made.

The graphite fibers were then dipped into a commercial borosilicate solution (Emulsitone Corporation, New Jersey) and placed under an infrared heat lamp. The solution dries to a glass-like material which is rich in boron. This coating process is similar to one widely used in the semiconductor industry.

The boron fibers were coated with a proprietary carbon slurry (CTS Corporation, Elkhart, Indiana) which air dries to an adherent coating. Although other carbon sources are of interest, none were investigated.

The coated fibers were placed in grooves in a quartz slide which was then inserted into the furnace. Of course, the graphite and boron fibers were never mixed and separate quartz tubes were used for each to avoid cross contamination of impurities which build up on the walls of the tubes.

The tube endcap was then replaced, the thermocouple moved into position and the entire system flushed with either nitrogen or argon (each was used at first but argon was used exclusively in the later experiments) for 30 minutes before the resistive heating elements were excited. The temperature was then raised at a rate limited only by the capabilities of the power supplies and the samples were held at elevated temperatures for various times.

The temperature was then decreased by reducing the current in the heating element and the transition to room temperature normally took from one to two hours. The inert gas continued to flow during this cool down process to avoid the introduction of impurities at the surfaces of the hot fibers. At the very least, the introduction of atmospheric oxygen would result in some oxidation of the fiber surfaces which would decrease the measured conductivities.

Once the fibers were removed, the residual coatings were etched using hydrofluoric acid. They were then rinsed in distilled water and methanol and dried in nitrogen and were then ready for attachment of electrical contacts as described in Sections 4 and 5.

The results of these diffusion experiments are summarized in the next section.

A brief investigation was also made of the intercalation of graphite fibers. This process is under investigation at the University of Pennsylvania<sup>19</sup> and optical data for intercalated graphite indicates conductivities comparable to that of copper. The intercalation process involves the introduction of large quantities of super acid radicals into graphite where the radicals act as electrical acceptors thereby increasing the density of mobile positively charged holes. It is unlikely that this process would produce fibers suitable for advanced composite materials because of the corrosive effect of the acid upon the integrity of the fiber-matrix bond which is critically important if the mechanical strengths of composites are to be maintained.

Following published procedure<sup>19</sup>, graphite fibers were immersed in a mixture of antimony pentafluoride and hydrofluoric acid for various times. Resultant changes in mass density allowed the calculation of a stage number. This index, in crude terms, refers to the percentage of basal graphite planes which are filled with the super acid radicals. For example, a stage 1 intercalation implies that every basal plane has accepted as much acid as possible while a stage N intercalation implies that one out of every N planes is filled.

The first intercalations resulted in stage numbers in the range of 10 to 20 and, at such low acid concentration, no changes in electrical conductivity were observed. In a second set of experiments, stage 5 intercalations were achieved and observed electrical conductivity increased by a factor of 8 to a value of  $1.6(10^5)$  mhos/m. Although no mechanical testing was performed, an apparently significant reduction in strength of the intercalated fibers was observed in that such fibers were more prone to break under normal laboratory handling than were untreated fibers.

No significant expenditure of time was devoted to the intercalation process in view of the efforts presently underway at the University of Pennsylvania and the Naval Research Laboratory.

## 7) ELECTRICAL BEHAVIOR OF DIFFUSED FIBERS

The first set of diffusion experiments used borosilicate coatings on graphite fibers and involved times from one to twelve hours and temperatures from 600°C to 1200°C. Sixteen diffusions were carried out using four different times (1,2,6,12 hours) and four different temperatures (600°C, 800°C, 1000°C and 1200°C).

Significant embrittlement of fibers occurred in the diffusion cycles involving temperatures of 1000 and 1200°C. These fibers appear to retain some surface residue after the normal post-diffusion cleaning procedures. In terms of electrical behavior, the fibers diffused at temperatures above 800°C display large resistivities when initially examined. When a pulsed electric field of about three hundred volts per centimeter was applied, the resistivity of the fibers dropped dramatically and reaches a value of approximately 50 percent of the pre-diffusion value. Fibers diffused at the lower temperatures (600 and 800°C) are electrically linear and display conductivities which are somewhat greater than the starting fibers themselves. This increase in conductivity was as large as a factor of five in a few fibers and, in others, as small as ten percent.

Nitrogen was used as the diffusion furnace gas in this set of experiments and another set was carried out over the same range of temperatures and times using argon. A borosilicate compound was again used as a source of boron as described previously. The results were essentially equivalent to those observed with nitrogen. Significant fiber embrittlement was observed at the highest diffusion temperatures, conductivity enhancement was clear in many samples, and some residual coatings remained after chemical etching.

A literature survey was conducted in an attempt to identify the compound which might be forming on the surfaces of the fibers.  $BN_4$  is a possible candidate because it is insoluble in acids. To check this hypothesis, graphite fibers were immersed in fused NaCl held at a temperature of  $801^{\circ}C$ . The time of immersion was 10-30 seconds. The fibers were electrically linear after this treatment and displayed no evidence of a surface residue. It was felt that the use of borosilicate as a source of boron impurity atoms, although successful in improving conductivity, leads to the formation of chemically resistant coatings which are removable in fused alkalis. The experimental difficulties involved in this procedure induced a search for alternate sources of boron for the diffusion experiments.

A boron nitride (BN) source was purchased from Materials Research Corporation and placed into the diffusion tube upstream (in terms of a gas flow) from the quartz slide carrying the graphite fibers. The boron atoms released from the heated boron nitride are carried along in the gas stream and provide a boron rich layer at the surface of the fibers. A set of experiments using this source was carried out at temperatures of  $600$  and  $700^{\circ}C$  for periods of three and six hours. In all cases, the increases in graphite conductivity were between 20 and 50 percent.

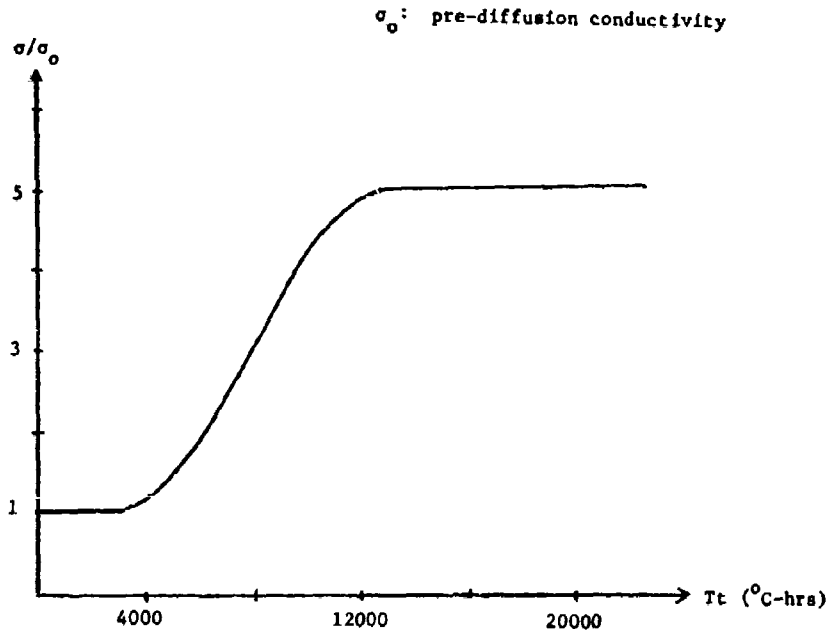
Another set of experiments was carried out for temperatures up to  $1200^{\circ}C$  for times as long as 20 hours. In no case were conductivity increases greater than the factor 5 observed.

This was surprising because it had been anticipated that increased diffusion times would lead to increased values of conductivity. There is some experimental evidence that the impurity species will occupy interstitial locations to a high degree if the diffusion temperatures are below  $2000^{\circ}C$ . It is likely that the factor of five improvement in conductivity which has been observed is the natural limit for impurities diffusing at relatively low temperatures. The disorder in the graphite fibers may be such that substitutional positions can be occupied by impurity atoms in large numbers only if the diffusion temperatures are high. The equipment precluded testing this idea because the quartz used as a furnace tube placed an upper bound of  $1300^{\circ}C$  on the operating temperature.

Figure 15 summarizes the conductivity enhancements observed in this first set of experiments.

To obtain higher diffusion temperatures, it was necessary to design and construct a small induction heated furnace. This furnace was capable of obtaining temperatures of  $2800^{\circ}C$  and was made operational in the last month of the contract period. It produced encouraging results in the first set of

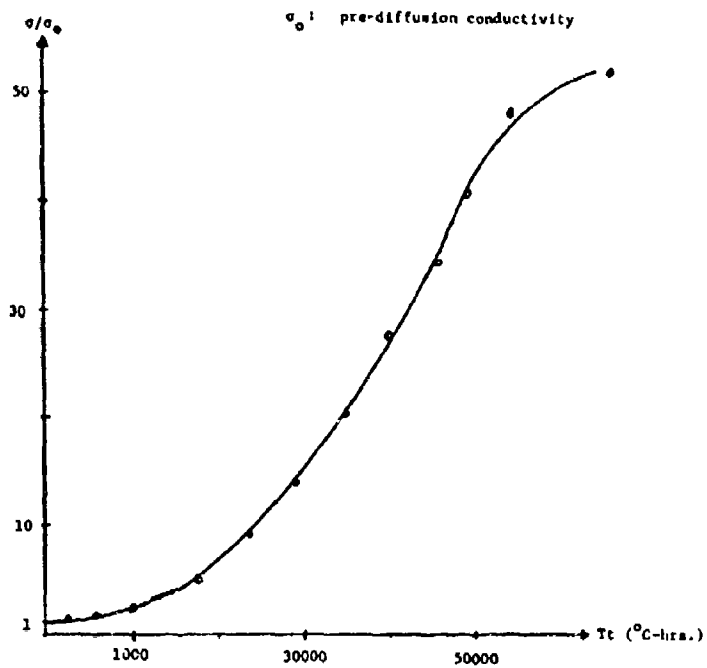
experiments. These are summarized in Figure 16. For some fibers, conductivities of  $1(10^6)$  mhos/m were measured.



CONDUCTIVITY ENHANCEMENT IN GRAPHITE

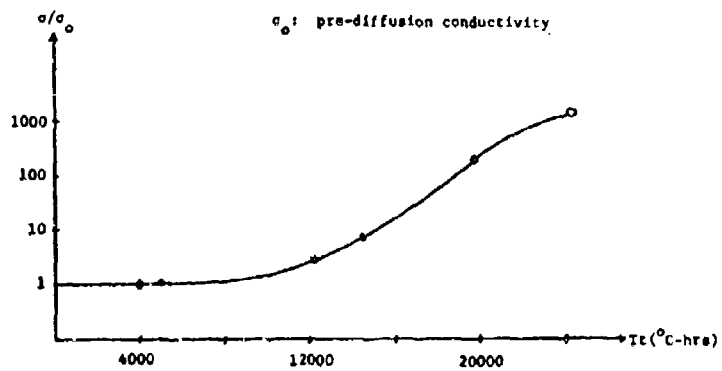
FIGURE 15

In view of the extended difficulties in making ohmic electrical contacts to the boron fibers, only preliminary diffusion experiments could be carried out. In all cases, the quartz diffusion furnace with an argon atmosphere was used. The first experiments were conducted at diffusion temperatures of 1000 and 1200°C for times of four, twelve, and twenty hours. These results are summarized in Figure 17.



CONDUCTIVITY ENHANCEMENT IN GRAPHITE  
HIGH TEMPERATURE

FIGURE 16



CONDUCTIVITY ENHANCEMENT IN BORON

FIGURE 17

## 8) SUMMARY OF RESULTS AND CONCLUSIONS

The activities during this contract period have led to two significant conclusions. The conductivities of graphite/epoxy and boron/epoxy advanced composite materials depend primarily upon the conductivities of the reinforcing fibers and the degree of fiber contact. From this, it follows that the overall composite conductivities can be enhanced in a mechanically acceptable fashion only by increasing the fiber conductivities themselves. Second, the additions of boron to graphite fibers and carbon to boron fibers result in significant increases in fiber conductivities.

The effort begun this year will continue under the sponsorship of the Air Force Office of Scientific Research. The goals of this work are to develop better statistical models of current flow in advanced composite materials and to more thoroughly characterize the diffusion process itself. In particular, during the period covered by this report, there were no tools available to determine the precise distributions of impurities present in the fibers before and after the diffusion cycles. One of the goals of next year's program is to develop an inhouse capacity to grow both graphite and boron fibers so that the background impurity content can be minimized. In addition, the facilities of the National Research and Resource Facility for Submicron Structures at Cornell University will be used to measure the impurity profiles in fibers. This will be done using a Secondary Ion Mass Spectrometer which uses an ion beam to sputter material from a sample and then spectrographically determines the atomic content of the sputtered material. This tool will determine the material composition of fibers as a function of radial depth. In this way, precise values for the diffusion coefficients of impurities in graphite and boron will be determined.

## 9) ACKNOWLEDGMENTS

The following individuals associated with the Electrical Engineering Department of the University of Notre Dame contributed to this research: Prof. Richard Kwor, Prof. W. Strieder, C. Araujo, T. Holzschuh and W. Barrett.

In addition, the assistance of T. Schoenberg (AVCO), S. Cross (Hercules) and D. Black (Narmco) is gratefully acknowledged.

## APPENDIX A

### A-1 INTRODUCTION

This appendix briefly describes the technique of nickel plating as it was used to electrically contact boron fibers.

In Section I, the nickel plating bath used in this particular case is described. Section II summarizes the cleaning and plating procedures and, in the conclusion, the success of this technique is described.

### A-2 THE NICKEL PLATING BATH

The nickel plating solution used in this particular experiment is a Watts Bath. The main constituents of this bath are nickel chloride, nickel sulfate and boric acid. Nickel sulfate is the principal source of nickel ion in the Watts Bath. The concentration of the nickel sulfate determines the limiting current density and the plating rate. Consequently, this determines how much current can flow through the cathode (i.e., the boron fiber). Nickel chloride improves anode (i.e., nickel metal) corrosion and conductivity. Increasing conductivity is of practical importance in order to reduce the voltage necessary to produce the desired current density. Boric acid is the solution buffer and helps to produce smoother and more ductile deposits of nickel.

Sound deposition of nickel depends on other parameters besides the chemicals in the solution. Temperature, agitation, controlling of the pH level, anti-pitting reagents, optimal anode-cathode current densities and low contamination are all of importance.

The bath that is used in our particular case has the following composition and operation conditions:

Constituent	Quantity
Nickel Sulfate (NiSO <sub>4</sub> ·6H <sub>2</sub> O)	300 g/l
Nickel Chloride (NiCl <sub>2</sub> ·6H <sub>2</sub> O)	60 g/l
Boric Acid (H <sub>3</sub> BO <sub>3</sub> )	42 g/l
4% Sodium Hydroxide Solution (NaOH)	42 g/l
30% Hydrogen Peroxide	2.5 ml/l diluted in 200 ml of H <sub>2</sub> O
Activated Charcoal	2.4 g/l

<u>Operating Conditions</u>	<u>Range</u>	<u>Preferred</u>
Temperature	49° to 66°C	60°C
pH	3.5 to 5.0	4.5
Current density of anode	--	100 amp/m <sup>2</sup>
Current density of cathode	--	530 amp/m <sup>2</sup>

The following steps are typical in the preparation of 500 ml of solution:

- Day 1:
1. Fill a clean beaker with 500 ml of distilled water. Heat it up to 66°C.
  2. Add 150g nickel sulfate and 30g of nickel chloride.
  3. Add 4% sodium hydroxide until the pH is approximately 5.2; agitate vigorously.
  4. Add 30% hydrogen peroxide - 1.25 ml diluted in 100 ml of H<sub>2</sub>O. Stir.
  5. Add 1.2g of activated carbon, stir for 2 hours and allow solution to settle overnight.
- Day 2:
6. Filter all the carbon out.
  7. Add 2lg of boric acid (stirring continuously)
  8. Adjust pH to 4 with dilute CP graded sulfuric acid.

Finally, for the first plating job using this solution, it is better to use a dummy cathode (e.g. copper wire). Nothing has been said so far about the anode and specific characteristics are given in Section II. For our case, a 100% pure nickel anode is not necessary which makes the technique economically attractive.

### A-3 CLEANING AND PLATING PROCEDURES

In order to attain consistent results for every plating of boron fibers, cleaning of the fiber is of vital importance. Considering the small diameter of these fibers (e.g., 4 to 8 mils) any particle of foreign material at the surface of the fiber will be covered with nickel and give v-i measurements inconsistent with similar samples of boron fiber. In order to avoid this the following procedure is used:

- (1) Vapor degrease the sample with trichlorethylene for at least 5 minutes.
- (2) Run the fiber through acetone, methanol and distilled water.

- (3) Drop fiber in sulfuric acid for 5 minutes.
- (4) Run through distilled water.
- (5) Blow dry with prepurified nitrogen. (Do not use any paper cleaning).

Before plating, the current densities were calculated using the following relationship:

$$j_A S_A = j_C S_C = I_p$$

where  $j_A$  = current density of the anode

$S_A$  = surface area of the anode

$j_B$  = current density of cathode

$S_B$  = surface area of cathode

$I_p$  = plating current

Assuming  $j_A = .01A/cm^2$  (preferred value for best results) and  $i_C = .054A/cm^2$  the relation becomes  $S_A = 5.38 S_C$ . This immediately determines the ideal minimum size of the nickel metal anode.

For our case, in the range of different diameters of fibers and up to 20 cm long samples, the anode is immersed 3-4 cm. and the plating current is set to 6 ma.

By setting the temperature at  $60^\circ \pm 2^\circ C$ , the ph at 4.5,  $I_p = 6$  ma and lightly agitating, best results are attained.

#### A-4 CONCLUSIONS

The technique thus far described has proven to be a reliable method of contacting boron fibers. It is also an easy and economic way of depositing uniform sheets of nickel on the boron fibers. Further, controlled thickness and amount of plating area make it convenient to measure v-i characteristics and verify current flowing predictions on the basis of the sample's geometry.

#### REFERENCES

1. Penton, et. al., "The Effects of High Intensity Electrical Currents on Advanced Composite Materials," Naval Air Systems Command, Report U-4866 (1970).
2. D. Strawe, L. Pitszker, "Interaction of Advanced Composites with Electromagnetic Pulse (EMP) Environment," AFML-TR-75-141, AD-D011927 (1975).
3. C. Skouby, "Electromagnetic Effects of Advanced Composites," (ONR) Final Report, Contract N00014-74-C-0200 (1975).
4. L. Scruggs and W. Gajda, "Low Frequency Conductivity of Unidirectional Graphite/Epoxy Composite Samples," Proc. IEEE International Symposium on Electromagnetic Compatibility, Seattle (1977).
5. M. Beran, N. Silnutzer, "Effective Electrical, Thermal and Magnetic Properties of Fiber Reinforced Materials," J. Composite Materials, 5, 246-249 (1971).
6. M. Beran, "Use of Variational Method to Determine Bounds for the Effective Permittivity in Random Media," Nuovo Cimento, 38, 771 (1965).
7. R. Stratton, et. al., "Electromagnetic Properties and Effects of Advanced Composite Materials: Measurement and Modeling," Rome Air Development Center (1978).
8. A. Marchand, "Chemistry and Physics of Carbon," 7, Marcel Dekker, Inc., New York (1971).
9. W. Neff, K. Seiler, "Boron," 2, Plenum Press, New York (1965).
10. W. Gajda, "On Solutions to the Diffusion Equation," Solid State Electronics, 13, 1427 (1970).
11. J. Crank, "The Mathematics of Diffusion," Oxford Press, London, p. 4. (1955).
12. Ibid. p. 72
13. L. C. Walko, "Current Status of Composites' Vulnerability to Lightning," SRD-74-909 (1974).
14. F. A. Fisher, W. M. Fassell, "Lightning Effects Relating to Aircraft," AFAL-TR-72-5 (1972).
15. J. T. Kung, M. P. Amason, "Lightning Protection Concept for Advanced Composite Structures," IEEE International Symposium on Electromagnetic Compatibility, Washington (1976).
16. W. Gajda, P. Ajmera, "Sample Standardization in Measuring the Electrical Properties of Graphite/Epoxy Composites," submitted to J. Composite Materials.

17. R. B. Adler, et. al., "Introduction to Semiconductor Physics," J. Wiley and Sons, New York, p. 17 et. seq. (1974).
18. T. Schoenberg (Private Communication), Avco Corporation, Lowell, MA (1977).
19. F. L. Vogel, J. Mat. Sci. (in press).